

Oscillations of pseudo Dirac neutrinos and the solar-neutrino problem

C. Giunti

Istituto Nazionale di Fisica Nucleare, Sezione di Torino, I-10125 Torino, Italy

C. W. Kim and U. W. Lee

Department of Physics and Astronomy, The Johns Hopkins University, Baltimore, Maryland 21218

(Received 30 March 1992)

The oscillations of pseudo Dirac neutrinos in matter are discussed and applied to the solar-neutrino problem. Several scenarios such as both ν_e and ν_μ being pseudo Dirac neutrinos and only ν_e or ν_μ being a pseudo Dirac neutrino are examined. It is shown that the allowed region in the mass-mixing angle parameter space obtained by comparing the solar-neutrino data with the calculations based on the standard solar model and the Mikheyev-Smirnov-Wolfenstein effect is not unique. The results depend on the nature of neutrinos; for example, if both ν_e and ν_μ are pseudo Dirac neutrinos, the allowed region determined by the current solar-neutrino data does not overlap with that obtained in the usual case of pure Dirac or Majorana neutrinos.

PACS number(s): 12.15.Ff, 14.60.Gh, 96.60.Kx

The observation of solar neutrinos, combined with the standard solar model [1] and calculations of the Mikheyev-Smirnov-Wolfenstein (MSW) effect [2] can provide important clues to understanding the basic properties of neutrinos. Current data from Homestake [3], Kamioka [4], and Soviet-American Gallium Experiment (SAGE) [5] have already narrowed down considerably the allowed region in the mass-mixing angle parameter space.

Recently there has been a proposal [6] to explain the solar-neutrino problem by using the MSW effect with only one generation of pseudo Dirac [7] electron neutrinos with a large transition magnetic moment. Majorana neutrinos emerge naturally in most extensions of the standard model, but some models (see, for example, Ref. [8]) yield pseudo Dirac neutrinos, which were used, among others, to explain the solar-neutrino puzzle.

In this paper, we generalize the one-generation picture to the case of two generations and examine the consequences. In particular, it is shown that in the pseudo Dirac neutrino case the current data yield entirely different (nonoverlapping) allowed regions in the mass-mixing angle parameter space from those in the standard Dirac or Majorana neutrino cases.

The Dirac-Majorana mass matrix for the neutrino states ν_L^e and ν_R^e is given by

$$\begin{array}{c|cc} & \overline{\nu_L^e} & \nu_R^e \\ \hline \nu_L^e & m_L^e & M_D^e \\ \nu_R^e & M_D^e & m_R^e \end{array} \quad (1)$$

where M_D^e and $m_{L,R}^e$ are the Dirac and Majorana masses, respectively. The assumption that $m_L^e + m_R^e = 0$ leads to pseudo Dirac neutrinos generated by a mechanism similar to that originally discussed by Wolfenstein [7]. In the following we make the assumption that $M_D^e \gg |m_{L,R}^e|$ which also leads to pseudo Dirac neutrinos [9], i.e., two almost degenerate (in mass) left-handed neutrino states ν_i^e

and ν_2^e (with masses $m_1^e \sim m_2^e \sim M_D^e$) which are expressed as

$$\begin{aligned} \nu_1^e &= i \cos\theta_e \nu_L^e - i \sin\theta_e \overline{\nu_R^e}, \\ \nu_2^e &= \sin\theta_e \nu_L^e + \cos\theta_e \overline{\nu_R^e}, \end{aligned} \quad (2)$$

where the factor i guarantees the positivity of the mass eigenvalues. The mixing angle θ_e is given by

$$\tan(2\theta_e) = \frac{2M_D^e}{m_R^e - m_L^e}. \quad (3)$$

In our case $\theta_e \sim 45^\circ$ because $M_D^e \gg |m_{L,R}^e|$. Therefore, our pseudo Dirac neutrinos are special ones, with an almost 45° mixing angle. In general, however, pseudo Dirac neutrinos can have any mixing angle and whenever pseudo Dirac neutrinos are generated with one generation one has to introduce sterile neutrinos.

In the following, we assume that

$$10^{-11} \text{ eV}^2 \lesssim \Delta m_e^2 \equiv (m_2^e)^2 - (m_1^e)^2 \lesssim 10^{-7} \text{ eV}^2,$$

where the upper limit comes from a cosmological constraint [10] on the oscillation into sterile neutrinos and the lower limit is necessary in order to have a vacuum oscillation length much shorter than the Sun-Earth distance. In this case, during the Sun-Earth propagation, one-half of the initial flux of ν_L^e will be depleted due to the maximal (45° mixing) oscillations between ν_L^e and $\overline{\nu_R^e}$ when the time average is taken. Therefore, the ratio of the ν_L^e flux at the Earth and the initial flux is one-half for the SAGE (\mathcal{S}), Homestake (\mathcal{H}), and Kamioka (\mathcal{K}), experiments:

$$\mathcal{S} = \mathcal{H} = \mathcal{K} = \frac{1}{2}. \quad (4)$$

If neutrinos have magnetic moments large enough to induce a spin flip during their propagation in the magnetic field of the Sun [11], the ratios of the neutrino fluxes

are

$$\nu_L^e : \overline{\nu}_L^e : \nu_R^e : \overline{\nu}_R^e = \alpha : \frac{1-2\alpha}{2} : \frac{1-2\alpha}{2} : \alpha \quad (5)$$

with $0 \leq \alpha \leq 0.5$. Since α is related to the spin-flip probability P_{SF} as $\alpha = (1 - P_{\text{SF}})/2$, any deviation from $\alpha = 0.5$ is an indication that spin flips actually took place. The detection rates are then

$$\mathcal{S} = \mathcal{H} = \alpha, \quad \mathcal{H} = \alpha + 0.42 \frac{1-2\alpha}{2}, \quad (6)$$

where we have used $\sigma(\overline{\nu}_L^e e^-) \simeq 0.42\sigma(\nu_L^e e^-)$. Assuming that the standard solar model [1] gives the correct ν_L^e flux produced in the core of the Sun, the ratios of the observed fluxes and the initial flux are $\mathcal{H}_{\text{expt}} = 0.27 \pm 0.04$ [3], $\mathcal{H}_{\text{expt}} = 0.46 \pm 0.08$ [4], and $\mathcal{S}_{\text{expt}} = 0.15 \pm 0.27$ [5]. The range of the parameter α for which Eq. (6) explains the observed ratios is $0.29 \lesssim \alpha \lesssim 0.31$.

Now we generalize the above one-generation picture to the case of two generations and study its consequences. We assume that, before the mixing between the electron and muon sectors, the muon neutrinos are also pseudo Dirac particles, i.e., $M_B^\mu \gg |m_{L,R}^\mu|$ so that $\theta_\mu \sim 45^\circ$. The two almost degenerate ($m_1^\mu \sim m_2^\mu \sim M_B^\mu$) mass eigenstate muon-neutrino states ν_1^μ and ν_2^μ are given by

$$\begin{aligned} \nu_1^\mu &= i \cos\theta_\mu \nu_L^\mu - i \sin\theta_\mu \overline{\nu}_R^\mu, \\ \nu_2^\mu &= \sin\theta_\mu \nu_L^\mu + \cos\theta_\mu \overline{\nu}_R^\mu. \end{aligned} \quad (7)$$

In the muon-neutrino sector, we assume that

$$10^{-11} \text{ eV}^2 \lesssim \Delta m_\mu^2 \equiv (m_2^\mu)^2 - (m_1^\mu)^2 \lesssim 10^{-2} \text{ eV}^2,$$

where the upper limit is due to the cosmological constraint [10]. However, both the mixing angles among the muon neutrinos and $\Delta m_{e\mu}^2 \sim (M_B^\mu)^2 - (M_D^\mu)^2$ are left unknown. For simplicity, we assume that $\Delta m_{e\mu}^2 \gg \Delta m_e^2$, Δm_μ^2 and that the mass eigenstates are given by

$$\begin{aligned} \begin{pmatrix} \nu_1 \\ \nu_2 \\ \nu_3 \\ \nu_4 \end{pmatrix} &= \begin{pmatrix} c_\theta & 0 & -s_\theta & 0 \\ 0 & c_\theta & 0 & -s_\theta \\ s_\theta & 0 & c_\theta & 0 \\ 0 & s_\theta & 0 & c_\theta \end{pmatrix} \\ &\times \frac{1}{\sqrt{2}} \begin{pmatrix} i & -i & 0 & 0 \\ 1 & 1 & 0 & 0 \\ 0 & 0 & i & -i \\ 0 & 0 & 1 & 1 \end{pmatrix} \begin{pmatrix} \nu_L^e \\ \overline{\nu}_R^e \\ \nu_L^\mu \\ \overline{\nu}_R^\mu \end{pmatrix}, \end{aligned} \quad (8)$$

where $c_\theta \equiv \cos\theta_{e\mu}$ and $s_\theta \equiv \sin\theta_{e\mu}$. The mixing angle $\theta_{e\mu}$ is practically equivalent to the usual mixing angle between ν_e and ν_μ in the Dirac or Majorana cases. Also, in Eq. (8) the pseudo Dirac mixing angles θ_e and θ_μ have been approximated to 45° . The mass matrix in the weak basis M_W^2 is given by

$$M_W^2 = \begin{pmatrix} \overline{m}_{12}^2 c_\theta^2 + \overline{m}_{34}^2 s_\theta^2 + A_e & \Delta m_{12}^2 c_\theta^2 + \Delta m_{34}^2 s_\theta^2 & (\overline{m}_{34}^2 - \overline{m}_{12}^2) c_\theta s_\theta & (\Delta m_{34}^2 - \Delta m_{12}^2) c_\theta s_\theta \\ \Delta m_{12}^2 c_\theta^2 + \Delta m_{34}^2 s_\theta^2 & \overline{m}_{12}^2 c_\theta^2 + \overline{m}_{34}^2 s_\theta^2 & (\Delta m_{34}^2 - \Delta m_{12}^2) c_\theta s_\theta & (\overline{m}_{34}^2 - \overline{m}_{12}^2) c_\theta s_\theta \\ (\overline{m}_{34}^2 - \overline{m}_{12}^2) c_\theta^2 s_\theta & (\Delta m_{34}^2 - \Delta m_{12}^2) c_\theta s_\theta & \overline{m}_{12}^2 s_\theta^2 + \overline{m}_{34}^2 c_\theta^2 + A_\mu & \Delta m_{12}^2 s_\theta^2 + \Delta m_{34}^2 c_\theta^2 \\ (\Delta m_{34}^2 - \Delta m_{12}^2) c_\theta s_\theta & (\overline{m}_{34}^2 - \overline{m}_{12}^2) c_\theta s_\theta & \Delta m_{12}^2 s_\theta^2 + \Delta m_{34}^2 c_\theta^2 & \overline{m}_{12}^2 s_\theta^2 + \overline{m}_{34}^2 c_\theta^2 \end{pmatrix} \quad (9)$$

with

$$\begin{aligned} \overline{m}_{12}^2 &\equiv \frac{m_1^2 + m_2^2}{2}, & \overline{m}_{34}^2 &\equiv \frac{m_3^2 + m_4^2}{2}, \\ \Delta m_{12}^2 &\equiv \frac{m_2^2 - m_1^2}{2}, & \Delta m_{34}^2 &\equiv \frac{m_4^2 - m_3^2}{2}, \\ A_e &= A_{\text{CC}} + A_{\text{NC}}, & A_\mu &= A_{\text{NC}}, \\ A_{\text{CC}} &= 2\sqrt{2}G_F E N_e, & A_{\text{NC}} &= -\sqrt{2}G_F E N_n, \end{aligned} \quad (10)$$

where $m_1, m_2, m_3,$ and m_4 are the mass eigenvalues. The values of the effective mass squared in matter are shown in Fig. 1 for $\nu_1, \nu_2, \nu_3,$ and ν_4 and their antiparticles as functions of the matter density ρ . In Fig. 1 there are two MSW resonance regions R1 and R2 and two possible spin-flip resonance regions R1_m and R2_m in addition to the region R discussed in Ref. [6]. In the region R the maximal vacuum oscillations lead to the $\frac{1}{2}$ suppression of the ν_L^e flux, as discussed above.

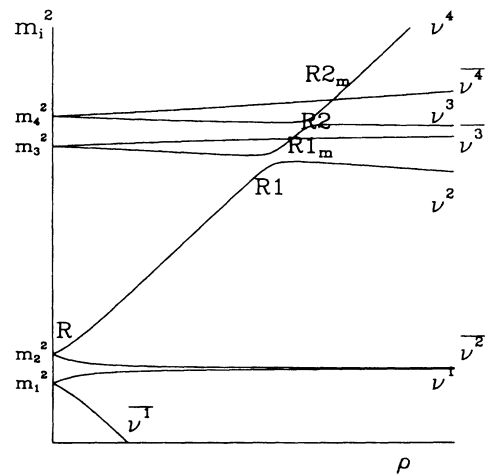


FIG. 1. Effective masses squared in matter for the energy eigenstates $\nu_1, \nu_2, \nu_3,$ and ν_4 as functions of the matter density ρ .

First we discuss the case in which neutrinos have large enough magnetic moments to induce resonant spin flips and the resonance regions $R1_m$ and $R2_m$ are in the convection zone. In this case the right-handed neutrinos $\overline{\nu}_L^e$, ν_R^e , $\overline{\nu}_L^\mu$, and ν_R^μ can be generated from the original ν_L^e by the resonant spin-flip processes directly or indirectly, e.g., via $\nu_L^e \rightarrow \nu_R^e$, $\nu_L^e \rightarrow \overline{\nu}_L^\mu$, $\nu_L^e \rightarrow \nu_R^\mu$, $\nu_L^e \rightarrow \overline{\nu}_L^\mu \rightarrow \nu_R^\mu$.

Regardless of whether or not the resonance spin-flip processes are adiabatic, the flux ratios at the Earth are expressed as

$$\begin{aligned} & \overline{\nu}_L^e : \overline{\nu}_L^\mu : \nu_R^e : \nu_R^\mu : \overline{\nu}_L^e : \overline{\nu}_L^\mu : \nu_R^e : \nu_R^\mu \\ & = a\alpha : a \frac{1-2\alpha}{2} : a \frac{1-2\alpha}{2} : a\alpha : b\beta : b \frac{1-2\beta}{2} : b \frac{1-2\beta}{2} : b\beta \end{aligned} \quad (11)$$

with $a+b=1$ and $0 \leq \alpha, \beta \leq 0.5$. The detection rates are then

$$\mathcal{S} = \mathcal{H} = a\alpha, \quad \mathcal{H} \simeq a\alpha + 0.21a(1-2\alpha) + \frac{1}{12}(1-a), \quad (12)$$

where we have used $\sigma(\nu_L^\mu e^-) \simeq \frac{1}{6}\sigma(\nu_L^e e^-)$ and $\sigma(\overline{\nu}_L^\mu e^-) \simeq \frac{1}{6}\sigma(\overline{\nu}_L^e e^-)$ instead of $\sigma(\overline{\nu}_L^\mu e^-) \simeq \frac{1}{7}\sigma(\overline{\nu}_L^e e^-)$ for simplicity. This approximation makes the second equation in Eq. (12) free of the parameter β . The results in Eq. (12) are consistent with $\mathcal{S}_{\text{expt}}$, $\mathcal{H}_{\text{expt}}$, and $\mathcal{K}_{\text{expt}}$ for the parameter ranges $a \gtrsim 0.93$ and $0.29 \lesssim \alpha \lesssim 0.31$ within 1σ . The fact that a must be very close to unity implies that the resonances $R1$ and $R2$ are extremely nonadiabatic in this model. Since the deviation from $\alpha=0.5$ indicates the presence of spin flip, the above range of α requires a large transition magnetic moment between ν_L^e and ν_R^e (e.g., $\sim 10^{-10}\mu_B$ for $B \sim 10$ kG in the convection zone). Although there exist many models that can yield such a large magnetic moment, they appear somewhat unnatural and thus we do not consider this scenario further.

In the absence of magnetic moments, no right-handed neutrinos are produced as ν_L^e ($\simeq \nu_4$ in the core) propagates outward from the core. At the resonance $R2$, ν_4 is split into ν_4 and ν_3 with fractions $(1-P_{R2})$ and P_{R2} , respectively, where P_{R2} is the Landau-Zener transition probability [12] at the resonance $R2$. At the resonance $R1$, the fraction P_{R2} of ν_3 is further split into ν_3 and ν_2 with fractions $(1-P_{R1})P_{R2}$ and $P_{R1}P_{R2}$, respectively, P_{R1} being the Landau-Zener transition probability at the resonance $R1$.

Let us assume that the two resonance regions do not overlap so that the two resonances can be treated separately. Then one can estimate the respective Landau-Zener transition probabilities as follows.

(1) *First resonance (R1)*. This is a resonance between ν_L^e and ν_L^μ and occurs when the first and third diagonal elements of M_W^2 are equal, i.e., for $A_{CC} = (\overline{m}_{34}^2 - \overline{m}_{12}^2)c_{2\theta}$. In the neighborhood of the resonance the MSW evolution equation is dominated by the $\nu_L^e - \nu_L^\mu$ 2×2 sector:

$$\begin{bmatrix} \overline{m}_{12}^2 c_\theta^2 + \overline{m}_{34}^2 s_\theta^2 + A_e & (\overline{m}_{34}^2 - \overline{m}_{12}^2)c_\theta s_\theta \\ (\overline{m}_{34}^2 - \overline{m}_{12}^2)c_\theta s_\theta & \overline{m}_{12}^2 s_\theta^2 + \overline{m}_{34}^2 c_\theta^2 + A_\mu \end{bmatrix}. \quad (13)$$

The Landau-Zener transition probability at the resonance is given by

$$P_{R1} = \exp \left[- \frac{\pi}{4h_{R1}} \frac{s_{2\theta}^2}{c_{2\theta}} \frac{\overline{m}_{34}^2 - \overline{m}_{12}^2}{E} \right] \quad (14)$$

with

$$h_{R1} \equiv \frac{1}{\rho} \left. \frac{\partial \rho}{\partial x} \right|_{R1}.$$

The mass factor in the exponent, $(\overline{m}_{34}^2 - \overline{m}_{12}^2)$, is equivalent to the usual $\Delta m_{e\mu}^2$.

(2) *Second resonance (R2)*. This is a resonance between ν_L^e and ν_R^μ and occurs when the first and fourth diagonal elements of M_W^2 are equal, i.e., for $A_e = (\overline{m}_{34}^2 - \overline{m}_{12}^2)c_{2\theta}$. In the neighborhood of the resonance the MSW evolution equation is dominated by the $\nu_L^e - \nu_R^\mu$ 2×2 sector:

$$M_W^2 = \begin{bmatrix} \overline{m}_{12}^2 c_\theta^2 + \overline{m}_{34}^2 s_\theta^2 + A_e & (\Delta m_{34}^2 - \Delta m_{12}^2)c_\theta s_\theta \\ (\Delta m_{34}^2 - \Delta m_{12}^2)c_\theta s_\theta & \overline{m}_{12}^2 s_\theta^2 + \overline{m}_{34}^2 c_\theta^2 \end{bmatrix}. \quad (15)$$

The Landau-Zener transition probability at the resonance is given by

$$P_{R2} = \exp \left[- \frac{\pi}{4h_{R2}} \frac{s_{2\theta}^2}{c_{2\theta}} \frac{\overline{m}_{34}^2 - \overline{m}_{12}^2}{E} \left[\frac{\Delta m_{34}^2 - \Delta m_{12}^2}{\overline{m}_{34}^2 - \overline{m}_{12}^2} \right]^2 \right] \quad (16)$$

with

$$h_{R2} \equiv \frac{1}{\rho} \left. \frac{\partial \rho}{\partial x} \right|_{R2}.$$

The ratio of the mass factors in the exponents of Eqs. (14) and (16) is

$$\begin{aligned} \left[\frac{(\Delta m_{34}^2 - \Delta m_{12}^2)}{(\overline{m}_{34}^2 - \overline{m}_{12}^2)} \right]^2 & \sim \left[\frac{\Delta m_{34}^2}{\overline{m}_{34}^2} \right]^2 \sim \left[\frac{M_D^\mu m_{L,R}^\mu}{M_D^{\mu 2}} \right]^2 \\ & \sim \left[\frac{m_{L,R}^\mu}{M_D^\mu} \right]^2. \end{aligned}$$

The numerical value of this ratio is supposed to be small for the pseudo Dirac neutrinos under consideration. Therefore, we take the nonadiabatic approximation for the resonant transition at $R2$. In order to see the region of validity for this approximation, let us consider the exponent of Eq. (16), which is written as

$$\begin{aligned} Q_{R2} & \simeq - \frac{\pi}{4} \frac{\sin^2(2\theta_{e\mu})}{\cos(2\theta_{e\mu})} \frac{R_\odot}{10.45} \frac{\Delta m_{e\mu}^2}{E} \left[\frac{m_{L,R}^\mu}{M_D^\mu} \right]^2 \\ & \simeq -2.6 \times 10^3 \frac{\sin^2(2\theta_{e\mu})}{\cos(2\theta_{e\mu})} \frac{\Delta m_{e\mu}^2}{\text{eV}^2}, \end{aligned} \quad (17)$$

where we have used $E=10$ MeV and for definiteness $m_{L,R}^\mu/M_D^\mu \approx 0.01$, which corresponds to the mixing angle $\theta_\mu=44.86^\circ$. The nonadiabatic region which satisfies $|Q_{R2}| < 1$ is below the solid line in the upper right-hand

corner in Fig. 2. It will be shown that the solution of the solar-neutrino problem in the pseudo Dirac neutrino model indeed lies in this region.

Therefore, one has the ratios of fluxes at the Earth,

$$\nu_L^e : \nu_L^\mu = \frac{1}{2} [P_{R1} \cos^2 \theta_{e\mu} + (1 - P_{R1}) \sin^2 \theta_{e\mu}] : \frac{1}{2} [P_{R1} \sin^2 \theta_{e\mu} + (1 - P_{R1}) \cos^2 \theta_{e\mu}], \quad (18)$$

leading to

$$\begin{aligned} \mathcal{S} &= \mathcal{H} = \frac{1}{2} \left[\frac{1}{2} - \frac{1}{2} (1 - 2P_{R1}) \cos(2\theta_{e\mu}) \right], \\ \mathcal{H} &= \frac{1}{12} + \frac{5}{12} \left[\frac{1}{2} - \frac{1}{2} (1 - 2P_{R1}) \cos(2\theta_{e\mu}) \right], \end{aligned} \quad (19)$$

where we have used the fact that, because of the maximal mixings between $\nu_L^e \leftrightarrow \nu_R^e$ and $\nu_L^\mu \leftrightarrow \nu_R^\mu$, only one-half of the neutrinos can be detected.

Treating P_{R1} as a constant parameter (neglecting the energy dependence of the transition probability), $\mathcal{S}_{\text{expt}}$, $\mathcal{H}_{\text{expt}}$, and $\mathcal{K}_{\text{expt}}$ are not reproduced by Eq. (19) within 1σ for any values of P_{R1} , but are reproduced within 2σ for

$$0.52 \lesssim \left[\frac{1}{2} - \frac{1}{2} (1 - 2P_{R1}) \cos(2\theta_{e\mu}) \right] \simeq 0.70. \quad (20)$$

The two-generation pseudo Dirac neutrinos discussed here are a special case of two-generation sterile neutrinos in which θ_e and θ_μ are 45° . Since the only mixing angle which is relevant in the analysis is $\theta_{e\mu}$, the above result should be compared with the usual MSW effect with two generations of neutrinos with the same mixing angle. In this case one has

$$\begin{aligned} \mathcal{S} &= \mathcal{H} = \frac{1}{2} - \frac{1}{2} (1 - 2P_{LZ}) \cos(2\theta_{e\mu}), \\ \mathcal{H} &= \frac{1}{6} + \frac{5}{6} \left[\frac{1}{2} - \frac{1}{2} (1 - 2P_{LZ}) \cos(2\theta_{e\mu}) \right] \end{aligned} \quad (21)$$

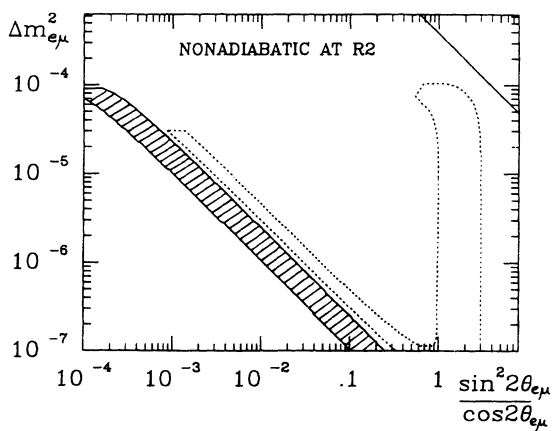


FIG. 2. $\Delta m_{e\mu}^2 - \sin^2(2\theta_{e\mu}) / \cos(2\theta_{e\mu})$ plots. The area inside the dotted line is the allowed region in the standard MSW effect, whereas the shaded area is the allowed region in the pseudo Dirac case. The transition at $R2$ becomes nonadiabatic in the region below the solid line in the upper right corner.

with the Landau-Zener transition probability P_{LZ} . Equation (21) can reproduce $\mathcal{S}_{\text{expt}}$, $\mathcal{H}_{\text{expt}}$ and $\mathcal{K}_{\text{expt}}$ within 1σ if

$$0.26 \lesssim \left[\frac{1}{2} - \frac{1}{2} (1 - 2P_{LZ}) \cos(2\theta_{e\mu}) \right] \lesssim 0.31$$

and within 2σ if

$$0.19 \lesssim \left[\frac{1}{2} - \frac{1}{2} (1 - 2P_{LZ}) \cos(2\theta_{e\mu}) \right] \lesssim 0.35. \quad (22)$$

There is an important difference between Eqs. (19) and (21): In Eq. (19), there is an additional factor $\frac{1}{2}$ due to the pseudo Dirac nature of the neutrinos, i.e., ν_L^e and ν_L^μ oscillate into ν_R^e and ν_R^μ , respectively, with 45° mixing, depleting the active (to detection) neutrinos by one-half.

Since P_{R1} depends on the energy E and the SAGE, Homestake, and Kamioka experiments have different energy thresholds, P_{R1} can be different for \mathcal{S} , \mathcal{H} , and \mathcal{K} . Using the expressions for P_{R1} , we have plotted the $\Delta m_{e\mu}^2 - \sin^2(2\theta_{e\mu}) / \cos(2\theta_{e\mu})$ diagram in Fig. 2 for the pseudo Dirac MSW and the usual MSW effects based on $\mathcal{S}_{\text{expt}}$, $\mathcal{H}_{\text{expt}}$, and $\mathcal{K}_{\text{expt}}$. We have taken $\langle E \rangle = 2.0$ MeV, 7.5 MeV, and 10 MeV for \mathcal{S} , \mathcal{H} , and \mathcal{K} , respectively. The region which satisfies $\mathcal{S}_{\text{expt}}$, $\mathcal{H}_{\text{expt}}$, and $\mathcal{K}_{\text{expt}}$ within 2σ in the standard two-generation MSW effect [with Eq. (21)] is shown as the area inside the dotted lines in Fig. 2. The region which satisfies $\mathcal{S}_{\text{expt}}$, $\mathcal{H}_{\text{expt}}$, and $\mathcal{K}_{\text{expt}}$ within 2σ in the pseudo Dirac case [with Eq. (19)] is shown as the shaded area inside the solid lines in Fig. 2. It is important to emphasize here that the two allowed regions in the $\Delta m_{e\mu}^2 - \sin^2(2\theta_{e\mu}) / \cos(2\theta_{e\mu})$ plot based on the same data $\mathcal{S}_{\text{expt}}$, $\mathcal{H}_{\text{expt}}$, and $\mathcal{K}_{\text{expt}}$, do not overlap, even within 2σ errors, i.e., the two-generation pseudo-Dirac neutrinos produce different allowed regions from those based on the usual two-generation model.

As variations of the above pseudo Dirac neutrino scenario, we consider the following two cases: (i) The electron neutrino is a pseudo Dirac neutrino but the muon neutrino is an ordinary Majorana or Dirac neutrino. (ii) The electron neutrino is a Majorana or Dirac neutrino but the muon neutrino is a pseudo Dirac neutrino. In case (i) there is one MSW resonance region and the neutrino fluxes at the Earth depend on the corresponding Landau-Zener transition probability P_{R1} . By assuming a mixing between ν_μ and ν_2^e with mixing angle $\theta_{e\mu}$, we have

$$\nu_L^e : \nu_L^\mu = \frac{1}{2} [P_{R1} \cos^2 \theta_{e\mu} + (1 - P_{R1}) \sin^2 \theta_{e\mu}] : [P_{R1} \sin^2 \theta_{e\mu} + (1 - P_{R1}) \cos^2 \theta_{e\mu}] \quad (23)$$

leading to

$$\mathcal{S} = \mathcal{H} = \frac{1}{2} \left[\frac{1}{2} - \frac{1}{2} (1 - 2P_{R1}) \cos(2\theta_{e\mu}) \right], \quad \mathcal{H} = \frac{1}{6} + \frac{1}{3} \left[\frac{1}{2} - \frac{1}{2} (1 - 2P_{R1}) \cos(2\theta_{e\mu}) \right]. \quad (24)$$

When we neglect the energy dependence of the detection rates, there is a region which satisfies the three detection rates within 2σ uncertainties:

$$0.40 \lesssim \left[\frac{1}{2} - \frac{1}{2} (1 - 2P_{R1}) \cos(2\theta_{e\mu}) \right] \lesssim 0.70. \quad (25)$$

The allowed region is similar to the case in which both neutrinos are pseudo Dirac type [see Eq. (20)] since in both cases there is only one adiabatic MSW transition region.

In case (ii) there are two MSW resonance regions, but in the region $R2$ the transition is extremely nonadiabatic, i.e., $P_{R2} \simeq 1$. The neutrino fluxes at the Earth depend on the Landau-Zener transition probability P_{R1} . By assuming a mixing between ν_1^μ and ν_e with mixing angle $\theta_{e\mu}$, we have

$$\nu_L^e : \nu_L^\mu = [P_{R1} \cos^2 \theta_{e\mu} + (1 - P_{R1}) \sin^2 \theta_{e\mu}] : \frac{1}{2} [P_{R1} \sin^2 \theta_{e\mu} + (1 - P_{R1}) \cos^2 \theta_{e\mu}] \quad (26)$$

leading to

$$\begin{aligned} \mathcal{S} = \mathcal{H} &= \frac{1}{2} - \frac{1}{2} (1 - 2P_{R1}) \cos(2\theta_{e\mu}), \\ \mathcal{H} &= \frac{1}{12} + \frac{1}{12} \left[\frac{1}{2} - \frac{1}{2} (1 - 2P_{R1}) \cos(2\theta_{e\mu}) \right]. \end{aligned} \quad (27)$$

When we neglect the energy dependence of the detection rates, we find a region that satisfies the three detection rates within 2σ uncertainty as

$$0.24 \lesssim \left[\frac{1}{2} - \frac{1}{2} (1 - 2P_{R1}) \cos(2\theta_{e\mu}) \right] \lesssim 0.35. \quad (28)$$

This allowed region is similar to the case of the ordinary MSW result [see Eq. (22)]. Note that this case is different from the previous one and the case of both neutrinos being pseudo Dirac types because the electron neutrino flux is not depleted in half.

In summary, the allowed regions in the mass-mixing angle parameter space obtained from the SAGE, Homestake, and Kamioka experiments are very different depending on the particle content of the neutrino sector. For example, the region allowed when both ν_e and ν_μ are pseudo Dirac neutrinos is very different from the region allowed by the analysis based on the usual two-generation MSW effect. Consequently, in order to pin down the values of $\Delta m_{e\mu}^2$ and $\theta_{e\mu}$ from future solar-neutrino experiments, it is necessary to have a complete understanding of the neutrino sector, in particular whether or not sterile neutrinos actually exist, and if they do, what their nature would be and so on.

Finally, we conclude with some short comments on the apparent atmospheric neutrino puzzle and the neutrinoless double- β decay. First, the atmospheric neutrino puzzle is that [13]

$$\frac{\Phi_{\nu_\mu}^{\text{obs}} / \Phi_{\nu_\mu}^{\text{cal}}}{\Phi_{\nu_e}^{\text{obs}} / \Phi_{\nu_e}^{\text{cal}}} = \begin{cases} 0.65 \pm 0.08 \pm 0.06 & \text{Kamioka,} \\ 0.64 \pm 0.09 \pm 0.12 & \text{IMB,} \end{cases} \quad (29)$$

where $\Phi_{\nu_e, \nu_\mu}^{\text{obs}}$ and $\Phi_{\nu_e, \nu_\mu}^{\text{cal}}$ are the observed and calculated fluxes of atmospheric neutrinos, respectively. This puzzle can easily be solved in the scenario in which both ν_e and ν_μ are pseudo Dirac neutrinos, as mentioned in Ref. [6], or in scenario (ii) discussed above as long as the constraints $\Delta m_e^2 \lesssim 10^{-7} \text{ eV}^2$ and $10^{-4} \text{ eV}^2 \lesssim \Delta m_\mu^2 \lesssim 10^{-2} \text{ eV}^2$

are met. The upper limits are both due to the cosmological argument [10] and the lower limit for Δm_μ^2 is necessary in order to have an oscillation length much shorter than the radius of the Earth. In these scenarios, ν_μ is depleted in half simply because of its pseudo Dirac nature. Furthermore, a value $\Delta m_\mu^2 \sim 10^{-4} \text{ eV}^2$, which corresponds to an oscillation length equal to the Earth diameter for $E \sim 500 \text{ MeV}$, could explain the observed suppression of the flux of low-energy muon neutrinos and a value between 0.5 and 1 for the ratio given in Eq. (29). Note that, in the case in which both neutrinos are pseudo Dirac type, ν_e is not depleted because the oscillation length is much longer than the radius of the Earth due to the cosmological limit mentioned above. Second, as already discussed in the past [14], neutrinoless double- β decay rates are naturally suppressed because they become proportional to m_L^2 , for the pseudo Dirac neutrinos that we have discussed. This implies that nonobservation of neutrinoless double- β decay cannot automatically lead to the conclusion that the electron neutrino is a Dirac particle.

Note added in proof. After the submission of this paper, the first result of GALLEX has been published [P. Anselmann *et al.*, Phys. Lett. B **285**, 376 (1992)]. The inclusion of the GALLEX data in our analysis modifies the shapes of the allowed regions in Fig. 1. In fact the allowed region for the pseudo Dirac neutrino case discussed in this paper becomes considerably smaller. The qualitative result of the paper, however, still remains the same, i.e., the allowed region in the Δm^2 - $\sin^2(2\theta)$ plot depends on the nature of the neutrinos. If the errors of the GALLEX data become smaller than the present values while the present central value remains the same, the pseudo Dirac neutrinos discussed in the paper may be ruled out, although more general cases with arbitrary mixing angles cannot be eliminated.

C.G. wishes to thank the Department of Physics and Astronomy of The Johns Hopkins University, and C.W.K. wishes to thank the INFN, Sezione di Torino, and il Dipartimento di Fisica Teorica, Università di Torino, for the hospitality extended to them while part of this work was performed.

- [1] J. N. Bahcall and R. Ulrich, *Rev. Mod. Phys.* **60**, 297 (1988).
- [2] L. Wolfenstein, *Phys. Rev. D* **17**, 2369 (1978); S. P. Mikheyev and A. Y. Smirnov, *Nuovo Cimento C* **9**, 17 (1986).
- [3] R. Davis, in *Neutrino '88*, Proceedings of the XIIIth International Conference on Neutrino Physics and Astrophysics, Boston, Massachusetts, 1988, edited by J. Schneps *et al.* (World Scientific, Singapore, 1989), p. 518.
- [4] K. S. Hirata *et al.*, *Phys. Rev. Lett.* **65**, 1297 (1990); **65**, 1301 (1990).
- [5] A. I. Abazov *et al.*, *Phys. Rev. Lett.* **67**, 3332 (1991).
- [6] M. Kobayashi, C. S. Lim, and M. M. Nojiri, *Phys. Rev. Lett.* **67**, 1685 (1991).
- [7] L. Wolfenstein, *Nucl. Phys.* **B237**, 147 (1981).
- [8] R. N. Mohapatra and J. W. F. Valle, *Phys. Lett. B* **177**, 47 (1986); J. F. Nieves and P. B. Pal, Report No. LTP-018-LIPR (unpublished); U. Sarkar, *Phys. Rev. D* **35**, 1528 (1987).
- [9] S. M. Bilenky and B. M. Pontecorvo, *Yad. Fiz.* **38**, 415 (1983) [*Sov. J. Nucl. Phys.* **38**, 248 (1983)]; S. M. Bilenky and S. T. Petcov, *Rev. Mod. Phys.* **59**, 671 (1987).
- [10] R. Barbieri and A. Dolgov, *Phys. Lett. B* **237**, 440 (1990); K. Enqvist, K. Kainulainen, and J. Maalampi, *ibid.* **249**, 531 (1990).
- [11] L. B. Okun, M. B. Voloshin, and M. I. Vysotskii, *Zh. Eksp. Teor. Fiz.* **91**, 975 (1986) [*Sov. Phys. JETP* **64**, 446 (1986)].
- [12] L. D. Landau, *Phys. Z. Sovjetunion* **2**, 46 (1932); C. Zener, *Proc. R. Soc. London A* **137**, 696 (1932); E. C. G. Stueckelberg, *Helv. Phys. Acta* **5**, 369 (1932). Their result was applied to neutrino oscillations in W. C. Haxton, *Phys. Rev. Lett.* **57**, 1271 (1986); S. J. Parke, *ibid.* **57**, 1275 (1986). For a recent review, see T. K. Kuo and J. Pantaleone, *Rev. Mod. Phys.* **61**, 937 (1989).
- [13] K. S. Hirata *et al.*, *Phys. Lett. B* **205**, 416 (1988); D. Casper *et al.*, *Phys. Rev. Lett.* **66**, 2561 (1991); the data given in Eq. (29) have been quoted by A. K. Mann, in *Proceedings of the 4th International Symposium on Neutrino Telescopes*, Venice, Italy, 1992, edited by M. Baldo-Ceolin (University of Padua, Padua, 1992).
- [14] For earlier references, see, for example, S. T. Petcov, *Phys. Lett.* **110B**, 245 (1982); J. W. F. Valle, *Phys. Rev. D* **27**, 1672 (1983).